TRACKING A SUNSPOT

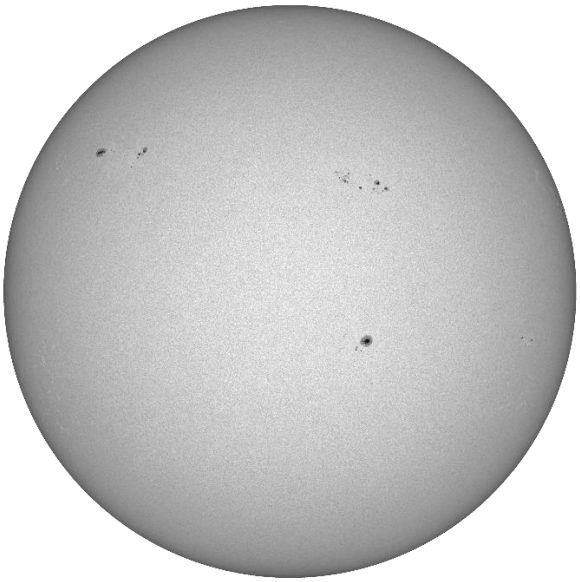

Figure 1 SDO/HMI Full disc Continuum intensity image

Mr. Leif Tinwell

Aberystwyth University

Physics with Planetary and Space Physics (B.Sc)

Third Year Project Dissertation

May 6, 2022

ABSTRACT

The torsional motions of sunspot AR 2939 were measured in detail for a period of 144 hours around a flare event thought to originate within this active region. The project made use of the high polling rates of the SDO/HMI instrument in order to yield complete and detailed measurements of the rotation. A Python programme was written to handle the substantial data set that came from the high polling rates used throughout the analysis. It was found that the sunspot umbra undergoes a reversal of rotation, and a harsh acceleration of its angular motion prior to the flare event. The flare occurrence seemingly halted the rotation of the umbra instantly. Although the umbra displayed strong motion, the penumbra was unaffected by the flare occurrence, and held a steady counter clockwise motion throughout the analysis, with only a small decrease in its angular motion thereafter the event. This differential rotation of the umbra and penumbra are yet to be understood correctly. It may constitute some straining mechanic on the flux tubes within a sunspot. This - when coupled with the rapid independent umbral acceleration - may inject sufficient magnetic energy stresses into the corona for an eruptive event to occur.

GENERAL AUDIENCE SUMMARY

Solar flares are energetic eruptive events that occur on the Suns surface and are largely responsible for adverse space weather near Earth. These events can cause great harm to the Earth and space-based technologies we so heavily depend on. They are known to drag satellites out of orbit, prevent radio communications and generate surges in our power grids, ultimately damaging them. In recent years, great progress has been made in understanding the physics of solar flares, though accurately predicting these events remains mysterious. As solar flares are thought to originate in active regions, the dynamics of the latter may ascertain vital information to the processes involved in such events. In this study, the rotation of a flaring sunspot was observed in hopes of correlating its dynamics to the flare phenomenon. Prior to the flare event, the sunspot was seen to reverse its rotation and suddenly accelerate. Upon flaring, the sunspot stopped rotating. This pattern of rotation may be observable in many other sunspots and may be indicative of the arrival of a flare.

ljt6@aber.ac.uk

CONTENTS

ljt6@aber.ac.uk

ljt6@aber.ac.uk

LIST OF FIGURES

ljt6@aber.ac.uk

ACKNOWLEDGEMENTS

First and foremost, I thank Mr. *Bray Gallienne,* for his collaboration in the research phase of the project. Although we went our separate ways during the experimentation phase, the preliminary cooperation he supplied was vital to the completion of the project.

I thank Dr. *Balázs Pintér,* project supervisor, for giving insight into the new frontiers of this field of research, providing his extensive understanding of sunspot dynamics and offering his theories and interpretations on some of the many unanswered questions. I would also like to acknowledge the astounding educational facilities and learning infrastructure Aberystwyth University has to offer, without which my interests in solar physics would not have developed into a burning passion.

Finally, I extend my gratitude to my cat, *Suki*, for his wonderful moral support and fluffiness.

ljt6@aber.ac.uk

1

Introduction

Sunspots are features on the photosphere which appear darker than the surrounding plasma due to their reduced temperature. This is a consequence of the intricate and intense magnetic fields that originate from the solar interior piercing through the photosphere and thereafter inhibiting subsurface convections that typically lead new hot plasma to the photospheric surface. The magnetic nature of sunspots has led to the general understanding that most of the solar surface activities are the product of the former, and that they largely govern the solar atmosphere. Therefore, atmospheric events, such as solar flares, are understood to typically originate from these active regions and their occurrence is related to the complexity of the magnetic fields comprising these regions. Solar flares and coronal mass ejections (CME) are the most energetic events in the solar atmosphere, but also our solar system, influencing a wide range of physical mechanisms on the solar surface, and outwards to space. These events are responsible for varying degrees of geomagnetic storms and can have detrimental effects on a plethora our technologies. Modern society is painfully dependent on Earth- and space-based technologies; the extent of the damage caused by solar flares and CMEs may be the advent of our downfall as an interconnected species. Advances in the ability to predict both are hence absolutely central to protecting Earth assets, namely GPS satellites, radio telecommunication, power grids and gas lines. The transport of magnetic energy from the solar interior and its storage in the corona seem to be the product of complex dynamics of active regions. [Moreover, these dynamics may be a display of the emerging magnetic patterns.] Although the conditions necessary for the occurrence of flares are unknown, there is clear evidence that sunspot dynamics are tightly kindred to flare activity; a study by which the dynamics of flaring sunspots are identified and measured may help corroborate their relation, and lead to better prediction.

A project was conducted to identify, track, and measure the dynamics of active regions on the solar disc. The work consisted of measuring the radial motions of a flaring sunspot, in an attempt to demonstrate a correlation between torsion within a sunspot and flare occurrence. The method involved acquiring *Solar Dynamics Observatory* (SDO) *Helioseismic and Magnetic Imag*er (HMI) data with high polling rate. The processing and analysis were done with a written python programme, in which the boundaries of a sunspot were extrapolated using intensity thresholds, and the orientations of the latter were measured for each image of the sequence. This provided a simple but nevertheless efficient and effective way to automatically measure sunspot rotation with a great deal of detail.

ljt6@aber.ac.uk

2

Literature Review

This literature review was the joint effort of the author and the collaborator and has been included for completeness.

2.1

Introduction

The focus of this project is to investigate characteristics of sunspots, in hopes of correlating solar properties and phenomena, by tracking them over some time period. As such, a number of fundamental questions are to be resolved ‘How do sunspots manifest solar magnetic activity’, ‘what are the processes involved in the formation of sunspots’, ‘what properties are connected within a sunspot’ and finally ‘How do sunspots correlate to solar atmospheric events’.

In this review, basic questions are to be answered and some insight into previous and current research on sunspots is to be given, along with a preliminary overview of the foreseen methodology to our project.

The premise for completing the project is entirely based on acquiring, processing, and analysing data. Such a practice requires a streamlined approach, establishing a database of images from SDO/HMI in the first place, then processing and plotting the data using SSWIDL. A quasi-automated approach is vital for generating large unbiased samples of sunspots in order to understand their contribution to solar activity.

2.2

Sunspots

2.2.1 Introduction

Sunspots are the most obvious feature on the disturbed photosphere and appear to play a key role in major solar events. They manifest the complexity of magnetic activity of the solar interior, witness the operation of solar dynamo deep in the convection layer, and define the frequency of solar cycles.[1, 2]

2.2.2 Lifecycle

The differential rotation of the Sun is its rotation around its axis. At the poles, the rotational period is approximately 40 days, and at the equator, 27 days (which indicates a rotational speed of 2 km s-1).

After a solar minimum, sunspots suddenly appear at ~40° latitudes (rotational period

ljt6@aber.ac.uk

of this location is 31 days). As the solar cycle progresses, they appear to drift towards the equator. At the next solar minimum, the sunspots (which will have reached the equator) disappear. Latitude migration of sunspots has no statistical difference between hemispheres. [3]

2.2.3 Underlying Physics

The coalescence of 3 or 4 small scale magnetic flux tubes proves to be sufficient in producing a cool area on the surface of the photosphere, described as a pore. These are distinguished from sunspots by their lack of a penumbra. In some cases, the magnetic knots move up towards the surface along field lines and merge with the pore. A penumbra (Fig.3.2-1) is formed when the magnetic configuration becomes unstable and the strongly inclined field interacts with the surrounding convective motions. [4]

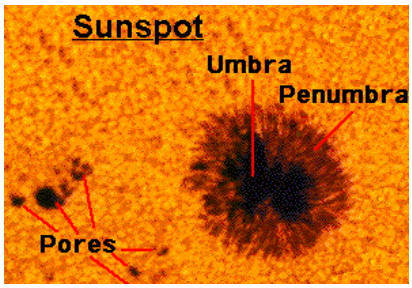

Figure 2.2-1 Sunspot areas

Observations have shown in the past [5] that sunspots are formed from the accumulation of small magnetic flux tubes (Fig. 3.2-2) at distances of general order of 10^3 km beneath the surface into a single magnetic flux tube. The motions of which are postulated to be driven by subsurface downdraft, depicted as dotted lines in Fig. 3.2-2, fed by inward horizontal flow from the surrounding region, dragging separate flux tubes into the sunspot. Once established, the convective force is thought to maintain the downdraft. [4]

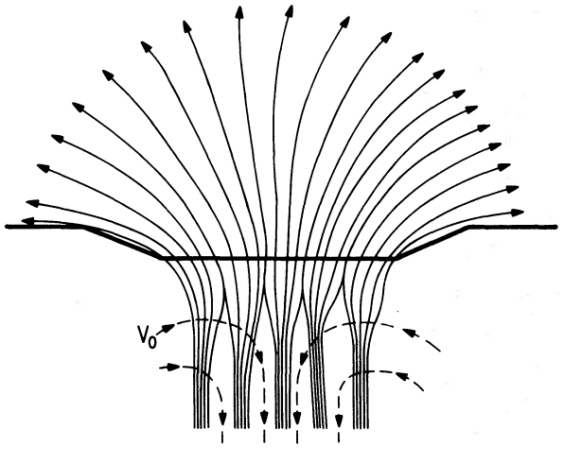

Figure 2.2-2 Diagram of sunspot flux tubes

From the centre umbra, the magnetic field strength systematically decreases from 0.3 T to about 0.1 T at the boundary of the penumbra, and then rapidly dies off. [6] Within the boundaries of the umbra, the field lines are vertical, with an increasing inclination outward. At the outer edge of the penumbra, the field lines flare outwards with an angle to the vertical of about 60° or more. Sunspots however are long-living magnetic structures, and hence they are stable for some extent of time. These flaring magnetic field lines at the surface are compressed by magneto-hydrostatic forces, its energy is enhanced, which would lead to instability. The question of how magnetic structures are made stable within a sunspot has been a long running puzzle in solar physics.

Meyer and Schmidt [7] suggest a formal criterion of the required conditions for stability: The surface of the flux tube is stable when confronted with the hydromagnetic exchange instability providing the flux tube diverges from the vertical by an angle θ larger than $\theta_0 \approx 20°$ for a common sunspot spanning 4 Mm across the umbra. Hence the usual observed 60° is rather larger than the θ_0 criterion, indicating that the visible portion of the sunspot is stable.

ljt6@aber.ac.uk

These intense vertical magnetic fields within a sunspot are generally accepted to inhibit the surrounding subsurface convective motions that transfer heat up to the photosphere. The resulting reduced temperature is observed as a dip in energy flux within the bounds of a sunspot. *Parker[4]* points out the amount of magnetic flux within a sunspot isn't sufficient to explain the extent of the observed 1/5th of the normal photospheric energy flux value. Measurements have shown sunspots to still be relatively hot, with an effective temperature in umbrae of about 4500 K and 5500K for the penumbrae. These observations lead to the assumption that convective energy transport is not completely suppressed. It is worth saying that the intensity contrast of sunspots with respect to the standard brightness of the photosphere is strongly wavelength-dependent. [1]

There are many characteristics of a sunspot to be understood and correlations to be made between each of their properties, but also to some of the sun's most fundamental mechanisms. Due to the magnetic nature of sunspots, it is clear that magnetogram observations will be one of the main focuses of this study. Also, due to the brightness and area of a sunspot being tightly kindred to the intensity of the magnetic structure, it would be wise to study the evolution of such properties. We shall also consider investigating the effects of sunspots on major solar events.

2.3 Sunspot & solar activity

2.3.1 Introduction

A general consensus has been established, ever since the discovery of the existence of magnetic fields in sunspots [8], that they have an important role in solar activity. [9] The extensive investigation of the structure and polarity of magnetic fields in solar active regions in later years have led to the understanding that at large scales, the evolution of magnetic fields are crucial to the solar activity cycle. The level of complexity of magnetic fields can be linked to energetic solar events such as flares and CMEs to solar flares; it is of general belief that the transport of magnetic energy from the solar interior and its storage in the corona seem to be the product of complex dynamics of active regions. [10] However, the understanding of how energy is stored and released is limited and the connections are purely empirical.

2.3.2 Causality between sunspot rotation and Solar flares, Coronal loops, CMEs

From numerous studies [11-13], it is widely accepted that flares derive their power from excess energy stored in stressed magnetic fields in active regions, such as sunspots. The details of the process of how the magnetic energy is explosively transformed into kinetic energy of coronal matter, however, requires more observational evidence, and remains an important issue in solar physics.

There seems to be several characteristics which favour the occurrence of flares, such as highly sheared magnetic fields [14] and the sudden change in the separation of two opposing polarities of active regions. [15] In this project, however, our attention will be turned towards the suggested

ljt6@aber.ac.uk

complicity of sunspot rotation with the energy build-up and release prior to flares.

Brown et al. [16] identified sunspot rotations in active regions using white light imagery from *TRACE*. Later *Tian et al.* [17] theorised the rotation of a sunspot twisted the corona, resulting in the generation of vertical helical currents within the solar atmosphere. More recently, *Xiao-Li Yan et al.* [18] emphasised the possible causality with flares by tracing the rapid rotation of a sunspot seemingly related to the X3.4 flare of 2006. By observing the evolution of NOAA 10930, a grouping of sunspots of negative polarity, the evidence was significant: There's an apparent correlation between the spatio-temporal characteristics of rotating sunspots and solar flares. Thus, the X3.4 flare was reasonably regarded as a result of the sunspot motions.

Xiao-Li Yan et al. [19] identified and classified rotating sunspots using *TRACE* and SOHO/MDI data. They found that there were some 60 possible different rotational patterns and found a strong relationship between these sunspots and flares. For sake of brevity, we will not be studying these different rotational patterns, however the data and relationships drawn in their study will prove to be invaluable to our project.

2.3.3 Coronal mass ejections

Solar eruptions are thought to be triggered by the magnetic shear stress exceeding a critical value, usually along a Polarity Inversion Line.

Observed sunspot rotation may be caused by photospheric flow or twisted flux tube emergence. The rotational motion can be the most dominant contributor to the magnetic field's twist and energy, which may contribute to how a flux rope system develops (which erupts as a CME).

Sunspot rotation may shear the footpoints of coronal magnetic field structures, causing magnetic reconnection between the low-lying flux rope and the overlying loop, which is thought to result in solar flares and coronal mass ejections. This process is theoretical, based on observations made on a major solar eruption in 2012. [20]

The area of the sun covered by sunspots has a correlation with the rate at which solar flares occur. The correlation between sunspot activity and coronal mass ejection rate is strongest with CMEs with speeds greater than the average speed. This suggests that sunspot associated CMEs are more energetic than those which originate elsewhere.

CMEs with speeds slower than average occur in all phases of the solar cycle. [21]

It was found that the activity cycle of CME slightly leads the sunspot area cycle close to the equator, but begins to significantly lag behind the sunspot area cycle as latitude increases. The cyclical behaviour of CMEs (where solar activity at low latitudes is in anti-phase to activity in high latitudes) supported existing ideas that CMEs are intrinsically associated with the magnetic structure. [22]

ljt6@aber.ac.uk

2.4

Observational Data

Data used in this project will be sourced from instruments on board the Solar Dynamics Observatory (SDO), specifically the Helioseismic and Magnetic Imager (HMI) as a means of capturing the complexities and evolution of active regions along the solar disk. The instrument is designed to produce four main types of data: Dopplergrams, continuum filtergrams, line-of-sight and vector magnetograms. [23]

In the first place, the continuum filtergrams (Fig. 3.4-1) will be used to track the visible properties of sunspots, such as their motions along the solar disk, the progression of their size, brightness, and rotation.

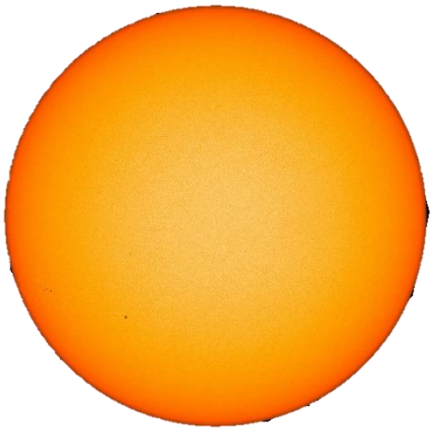

Figure 2.4-1 Continuum image

In second place, the magnetograms (Fig. 3.4-2) will be used to investigate the complex magnetic structures that arise from sunspots, to study their polarity and to quantify the change in magnetic fields prior to solar atmospheric events.

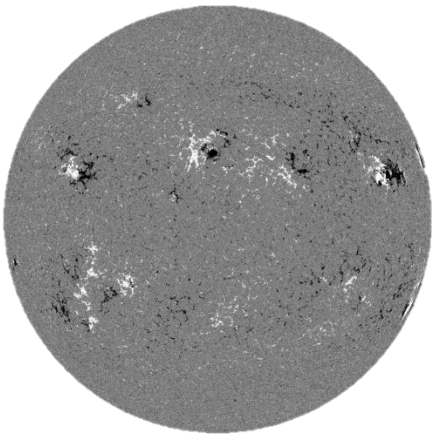

Figure 2.4-2Magnetogram

Eventually, the HMI data could be used in conjunction with the Atmospheric Imaging Assembly (AIA), which provides continuous observations (Fig. 3.4-3) of the solar chromosphere and corona under 10 different wavelengths, to identify plausible connections between the magnetic features of sunspots and their effects on the sun's atmosphere.

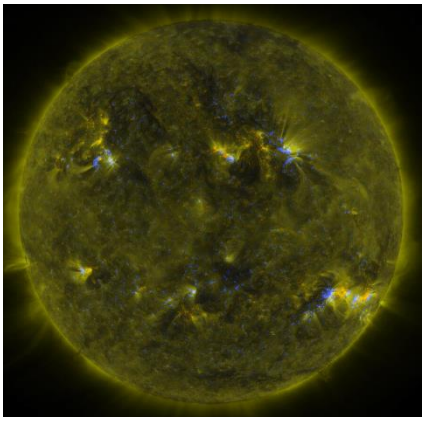

Figure 2.4-3 Composite AIA image

ljt6@aber.ac.uk

2.5 Automated tracking and processing methods

2.5.1 Processing data

Our SDO data will first be read and processed using SSWIDL, following the guidelines described in *Daniel Brown's* SDO primer. [24]

2.5.2 Tracking sunspot groups

L. Győri [25, 26] developed a method to track entities related to sunspot groups, based on graph operations.
The pixels of the first image in sequence are transformed into the pixels of the next image (Fig.3.5-1/2), using heliographic coordinates to account for differing scales and orientations.

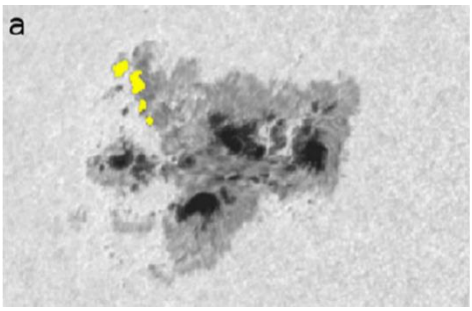

Figure 2.5-1

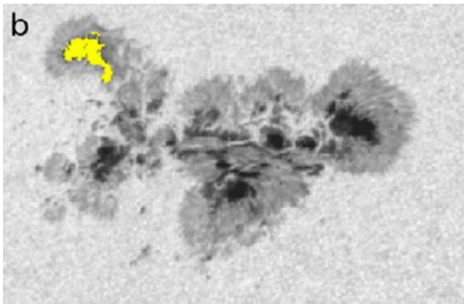

Figure 2.5-2

Relations are defined between entities in the images. Once completed for an image series, a chart is produced for each entity pair. Vertices represent entities in the images and the edges link to related entities in future images.
Iterating through families, the entities can be studied for merge and fragmentation events.

2.5.3 Tracking sunspot rotation

Another method was used by *B. Daniel and Walker A.* SDO continuum data is analysed by comparing numerous observations in a sequence. The centre of the sunspot in each image is identified (Fig. 3.5-3) and uncurled from cartesian coordinates to polar coordinates (Fig. 3.5-4).

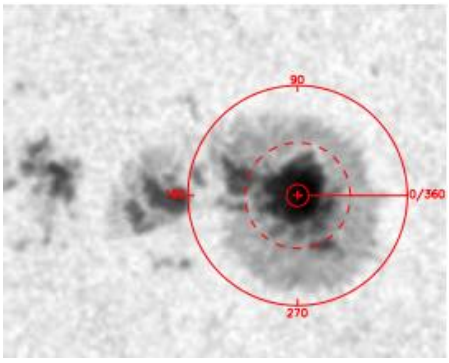

Figure 2.5-3 Sunspot with identified centre

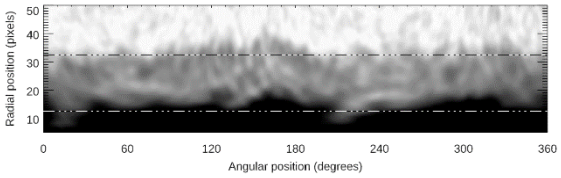

Figure 2.5-4 Unwrapped image of sunspot

The intensity profile of each radial band in the sunspot is investigated. Turning points are found, which will track rotational motion in the penumbra. Turning points are matched to equivalent ones in the previous observation, allowing for the change in rotation to be calculated between the two images, which can be divided by time to get rotational speed. [27]

ljt6@aber.ac.uk

The time-slice method can be used to determine the rotation rate of a sunspot as a function of time. Active regions are selected, with the image closest to the solar disk's centre chosen to minimise the projection effect.
To derive the rotational parameters of the sunspots, the centre of the umbra is followed. Determining the centre of the sunspot can either be determined by the maximum point on the magnetogram or the point of minimum intensity on a white-light image.
The sunspot image is uncurled by transforming from a cartesian frame of reference to a polar frame. This is to get the intensitygram of the sunspot in polar coordinates. Repeating for all images provides the θ variation as a function of time. [28]

2.5.4 Tracking movement and area

With a suitable image of a sunspot *ImageJ* can be used to determine the coordinates and area of a sunspot, and *Helioviewer* can be used to determine centre disk heliographic coordinates, position angle, and semi-diameter of the Sun. These parameters are then used to convert the pixel coordinates into heliographic coordinates.

By using linear regression, the equation of differential rotation can be found as a function of a sunspots age T, its longitudinal drift velocity dL and V_c the Carrington velocity:

$$\omega(\mathrm{B}) = \frac{(V_c\,\mathrm{T}) + \mathrm{dL}}{T}$$

It has been shown that the rotational velocity of a sunspot increases as it approaches the equator. [29]

2.6

Future directions

2.6.1 Atmospheric coupling

In the 1960's, *Leighton* and his team discovered that the photosphere oscillates, their explanation was that sound waves exist within the solar interior. [30] Studying these oscillations would bring forth properties of these waves, along with an understanding of the solar centre. It has been found that there are systematic variations in the frequency of different oscillation modes in time.[31] The time period of these shifts of frequencies is about 11 years, indicating that there is some correlation with magnetic effects going on. During the periods where the sun is more active, presenting more sunspots on the surface, the frequencies of global oscillations increase likewise. [32] The question is worth asking, how could the magnetic field present in the atmosphere interact with the global oscillations which are thought to exclusively exist in the solar interior?

Since these ground-breaking studies, there have been great improvements over the resolution of spatial and temporal data, allowing more detailed study of these oscillations present within the solar atmosphere. Sunspots might prove to be windows for studying helioseismology. [33]

ljt6@aber.ac.uk

2.7

Conclusion

The aim of this project is to closely investigate the motions and evolution of sunspot groups using SDO/HMI data, in the hopes of establishing our own correlations between their properties and relate them to some of the most intriguing solar atmospheric events. Following the processing and automatic tracking methods of both *L. Gyori* and *B. Daniel* will provide observational results which may offer answers to the projects focus. The literature on the motion and properties of sunspots was widely regarded as factual, however the same cannot be said for the literature concerning sunspot effects on events such as solar flares or CMEs. Most studies have been correlating magnetic properties and solar phenomena on an empirical basis.

ljt6@aber.ac.uk

3

Experimental Methods

The SDO/HMI continuum data provided the images of the sunspot. Each image was then corrected for limb darkening to ensure consistent pixel intensity across the entire solar disc, so as to precisely detect umbral and penumbral boundaries using intensity thresholds. Subsequently, the centre of mass of the sunspot was determined, and an ellipse was fitted to the boundaries. Any rotational motion with respect to the centre of mass of each region would then be detected as an angular displacement in the orientation from vertical of the ellipse's major axis.

3.1 Data

The method was developed to analyse sequences of continuum intensity images taken by the HMI module onboard *NASA*'s SDO. The instrument captures the photosphere at many different wavelengths; however, the continuum intensity observables are best suited for the study of sunspots. The hmi.*Ic_45s* series provides images of the surface of the sun in the spectral region of the 6173 Å FeI absorption line – white light – at a maximum cadence of 45s. As typical rotation rates of a sunspot are in the range of 0-3° per hour, or up to 0.15° per 3 minutes, a polling rate of 1 image every 3 minutes was selected. This rate struck an adequate balance between limiting data weight and yielding ample detail in the measurements.

For the study case, sunspot AR2939 was preselected using the *Solar Demon Flare Detection* [34] data base, which provides an exhaustive list of all flare detections. AR2939 was associated with several C-class flares while visible on the solar disc, which constituted the basis of its selection. Then, a preliminary survey of the sunspot's features was carried out using *JHelioviewer*. The active region was identified as the perfect test candidate for several factors: Its proximity to the solar equator limited the distortion of its image during its travel across the disc, its size, shape, and clarity simplified the boundary detection methods, and altogether was a well-behaved sunspot.

ljt6@aber.ac.uk

3.2 Acquiring Data

The *SunPy* DRMS Python [35] package provided the framework to construct queries and submit requests to the *Data Record Management System* (DRMS) database developed by the *Joint Science Operation Centre* (JSOC). The database centre handles the processing of SDO's HMI and AIA instrument products and manages their distribution. DRMS records are selected by creating query strings that contain the series name (*hmi.Ic_45s)*, followed by the time interval and polling rate of the requested observations. Sunspot AR2939 was tracked for 6 days from the 2nd to the 8th of February earlier this year, detailing over 2500 images. When considering large datasets, it is fundamental to implement methods to reduce file size to a minimum in order limit download and processing times. Hence, cut-outs of sunspots were requested in place of full disc images, shrinking the file size from 16 MB to less than 100 KB for each image in the sequence.

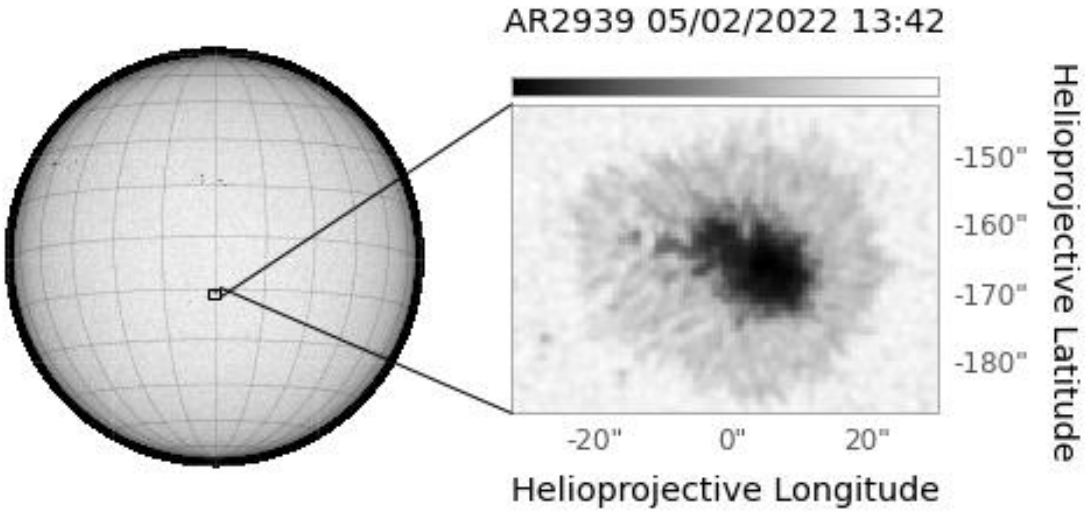

Figure 3.2-1 HMI cut-out

To do so, the coordinates of a bounding box of 50 arcsec was estimated (Fig. 3.2-1) around the approximate centre of the sunspot as it passed solar centre on the 5th at 13:42 UT using *JHelioviewer*. A cut-out request using the bounding box coordinates was constructed and sent to the JSOC server, which then returned the associated files tracked across the solar disc for the duration of the analysis. The files were then sent through a processing pipeline to remove the effects of limb darkening.

ljt6@aber.ac.uk

3.3 Limb Darkening Processing

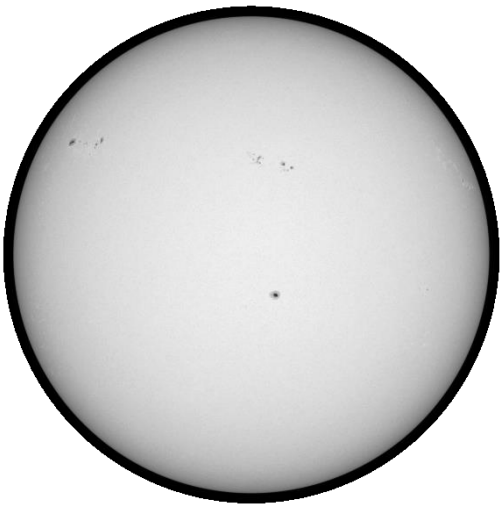

Figure 3.3-2 Limb darkened solar disc

Figure 3.3-1 Limb corrected solar disc

Limb darkening (Fig. 3.3-2) is a visible artifact of the systematic variations in intensity across the solar disc due to decreasing optical depth towards its edges. Some processing to remove these effects was essential to accurately determine sunspot boundaries using pixel intensities. The correction ensured consistent sunspot brightness across the solar disc (Fig. 3.3-1) and allowed the use of fixed threshold values, while removing any noise and intensity fluctuations within the boundaries of the sunspot, further aiding the detection of the latter. The script is largely based on the limb darkening function available in IDL/SSW [36]. It makes use of many of the .FITS file headers and suits a 5^{th} order polynomial to the limb darkening coefficients obtained from Astrophysical Quantities [37].

ljt6@aber.ac.uk

3.4 Determining Umbral and Penumbral Boundaries

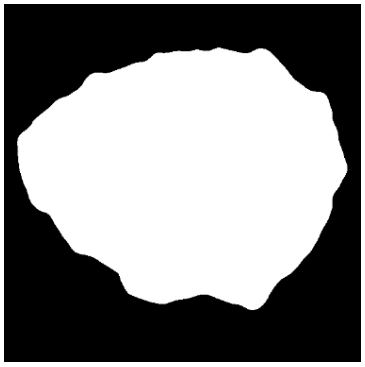

Figure 3.4-1 Penumbral threshold binary image

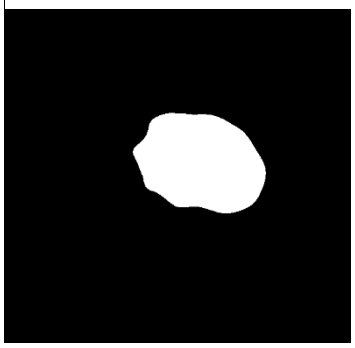

Figure 3.4-2 Umbral threshold binary image

Once the data sequence was corrected for limb darkening, it was then passed through a Gaussian filter to smooth umbral and penumbral boundaries, remove leftover granularity and unwanted variations in pixel intensities within these areas. Doing so increased efficacy and accuracy in the following procedures. Subsequently, the umbral and penumbral areas were determined by applying a set of binary threshold operations to the limb corrected and filtered images of the sequence. The threshold values used in these procedures were predefined as ratios of the average intensity of the solar disc for every image; any eventual localised brightening of boundary pixels caused by temporary disruptions in the photosphere would be adjusted for. To obtain the adequate intensity thresholds, the *DATAMEAN* header value from each .FITS file was extracted and multiplied by several scaling factors. The umbral-penumbral boundary was defined as 60% of the average full disc intensity, while the penumbral pixels were bound to]60%-130%] average disc intensity. This method can be extended to use a variety of smaller umbral intensity values to track the differential motions within the sunspot's umbra: This is the basis of the Multi-Layer Thresholding technique [38]. With these thresholds, the script produced a sequence of binary images (Fig.3.4-1 & 2) in which pixels with an intensity below the specified values were set to white; or black if the pixel intensity was greater than the threshold values.

This was done for both the umbral and penumbral ranges of threshold values, and hence determined their respective boundaries. The perimeters of each region were then drawn from the binary images and the corresponding centre of mass was computed as the mean location of the group of umbral and penumbral pixels, such that:

$$x_{cen} = \frac{1}{N}\sum_{k=1}^{N} x_k \qquad \text{and} \qquad y_{cen} = \frac{1}{N}\sum_{k=1}^{N} y_k$$

Where pixels have locations given by (x_k, y_k) where $k = 1, \dots, N$ with N the total number of pixels in the grouping. A least-squares ellipse fit [39] was performed around both umbral and penumbral boundaries (Fig. 3.4-3) using the calculated centre of masses and the orientation of the major axis relative to the solar equator was recorded for each image in sequence. The programme then plotted the rotation data as a function of time.

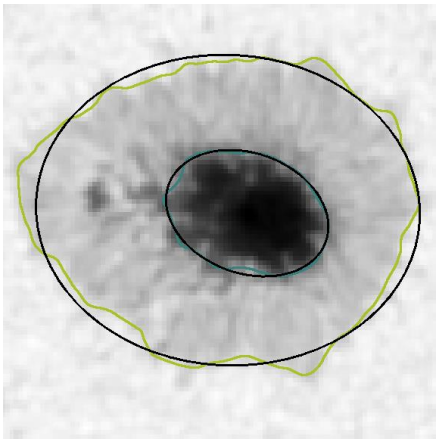

Figure 3.4-3Ellipses fitted to contours

ljt6@aber.ac.uk

4

Results

4.1 AR 2939

Sunspot AR2939 was analysed within 45° either side of solar centre from the 2nd February 2022 09:20 UT to the 8th February 2022 00:00 UT. The average *DATAMEAN* value obtain from the sequence was 43165.6 DN, defining an umbral-penumbral boundary threshold of 23191.1 DN (120 Grayscale value) and a penumbral upper boundary of 49775.4 DN (215 Grayscale value). A C2-class solar flare was recorded within the active region between 13:06 and 14:56 UT on the 6th February 2022, foretelling compelling dynamics to be studied.

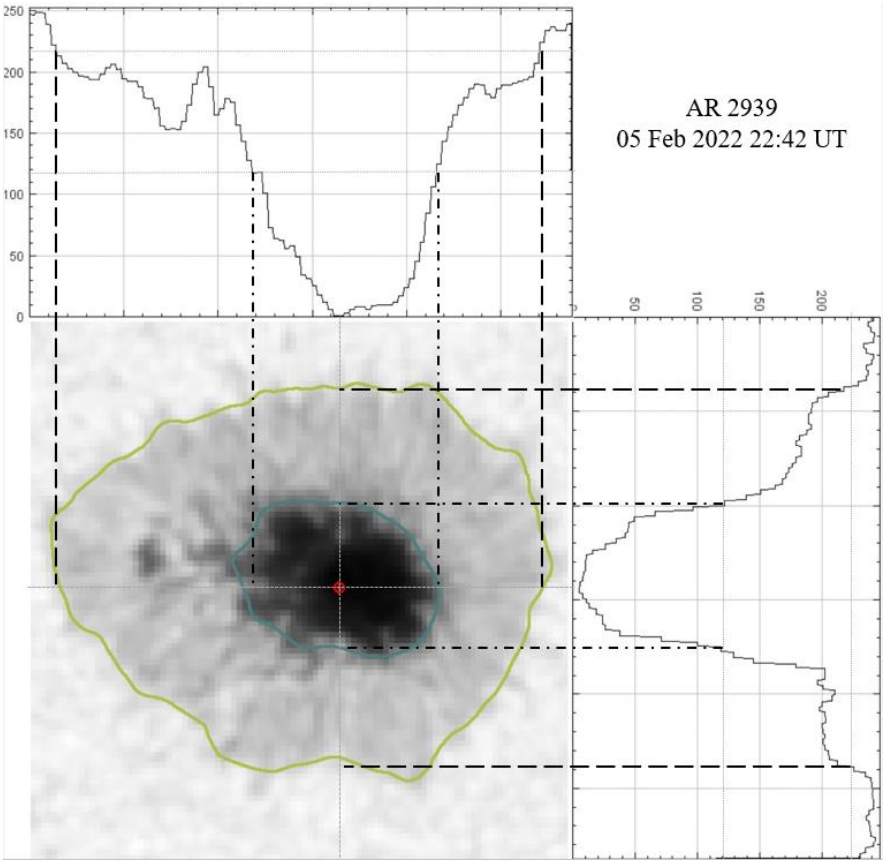

A limb corrected image of the sunspot is shown in Figure 4.1-1, along with intensity profiles taken through the centre of the sunspot across the horizontal and vertical. The calculated umbral penumbral thresholds are plotted on the intensity profiles, and the boundaries are drawn.

Figure 4.1-1 Limb corrected sunspot with intensity profiles

ljt6@aber.ac.uk

4.2 Area

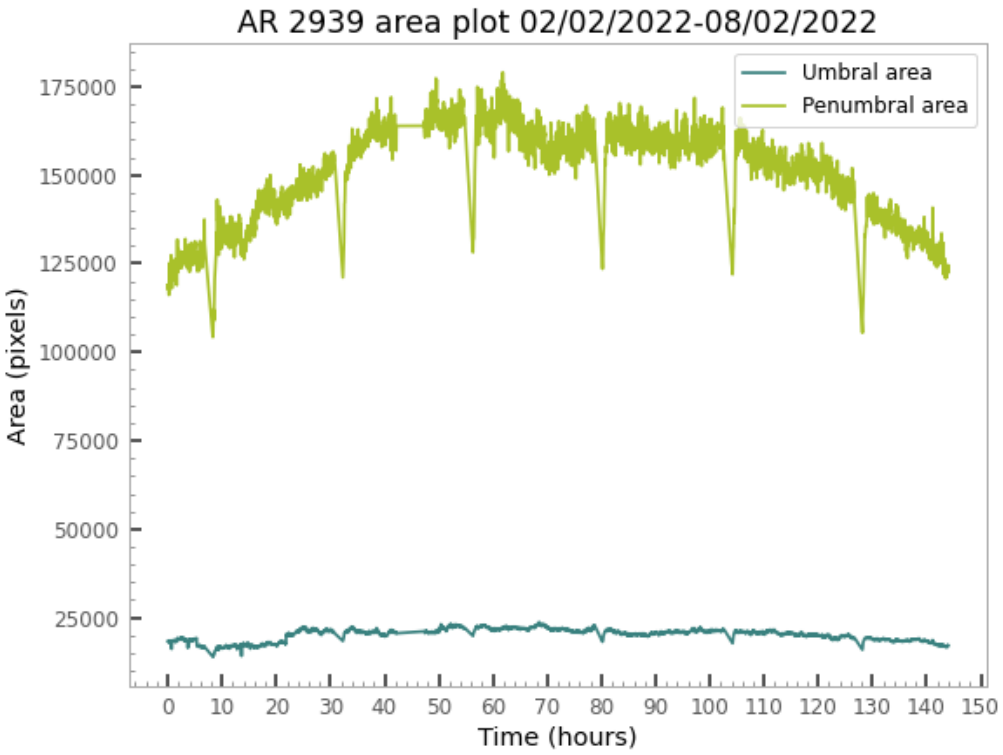

Figure 4.2-1 AR2939 Area plot

The first output of the programme is a plot of the pixel area as a function of time in hours (Fig. 4.2-1). The umbral and penumbral area are measured with a polling rate of 1 image every 3 minutes by means of the different thresholding values. The green curve relates to the penumbral area, while the blue to the umbral area. The periodic troughs are present in both data sets and are a consequence of the Earth occluding the SDO's line of sight for approximately 90 minutes each day. This happens for a period of a couple weeks every year near each equinox, it is unfortunate that the sunspot happened to be in this period. Nevertheless, the subsequent measurements of angular motions remain consequential. On the other hand, the curvature of the penumbral area plot – also present in the umbral area plot, albeit less exaggerated at this scale – is the reason for limiting the sunspot analysis to within 45° either side of solar centre. Fundamentally, the Sun and its sunspots are 3-dimensional objects being observed as a 2-dimensional image. As a sunspot approaches the solar limb, the perceived image will be increasingly distorted and eccentric. To extend analysis to the solar limb, a method of reprojecting the sunspot image to solar centre will need to be implemented. (This was unfortunately left out in respect of time constraints)

ljt6@aber.ac.uk

4.3 Penumbral Rotation

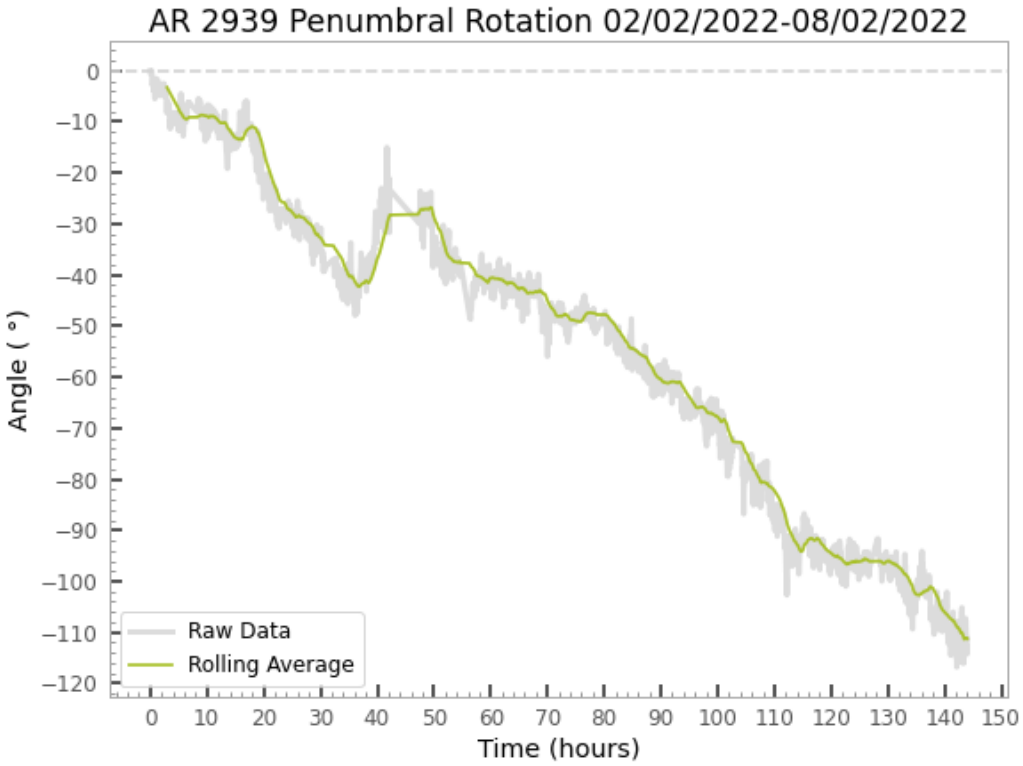

Figure 4.3-1 Penumbral rotation profile plot

Figure 4.3-1 shows the cumulative rotation profile of the ellipse fitted to the penumbral boundary plotted as a function of time in hours. Overall, the sunspot displayed a relatively constant counter clockwise (negative) rotation for the duration of the analysis. However, by virtue of the high polling rates, much of the detail in the rotation can be measured. A rolling average for every 60 data points was plotted for ease of visualising the rotation. In the first instances of the analysis, 0-39h, the penumbra rotated with a steady counter-clockwise motion, thereupon reversing its motion to that of a clockwise rotation (positive), until returning to the habitual negative rotation at 44h. It is worth noting that there is missing data between 42-48h. A slowing down of the angular motion occurs at 114h. This seems to coincide with the flare onset at 118h, though there does not seem to be much interaction or corelation with the solar flare on the 6th February 13:00 UT.

ljt6@aber.ac.uk

4.4 Umbral Rotation

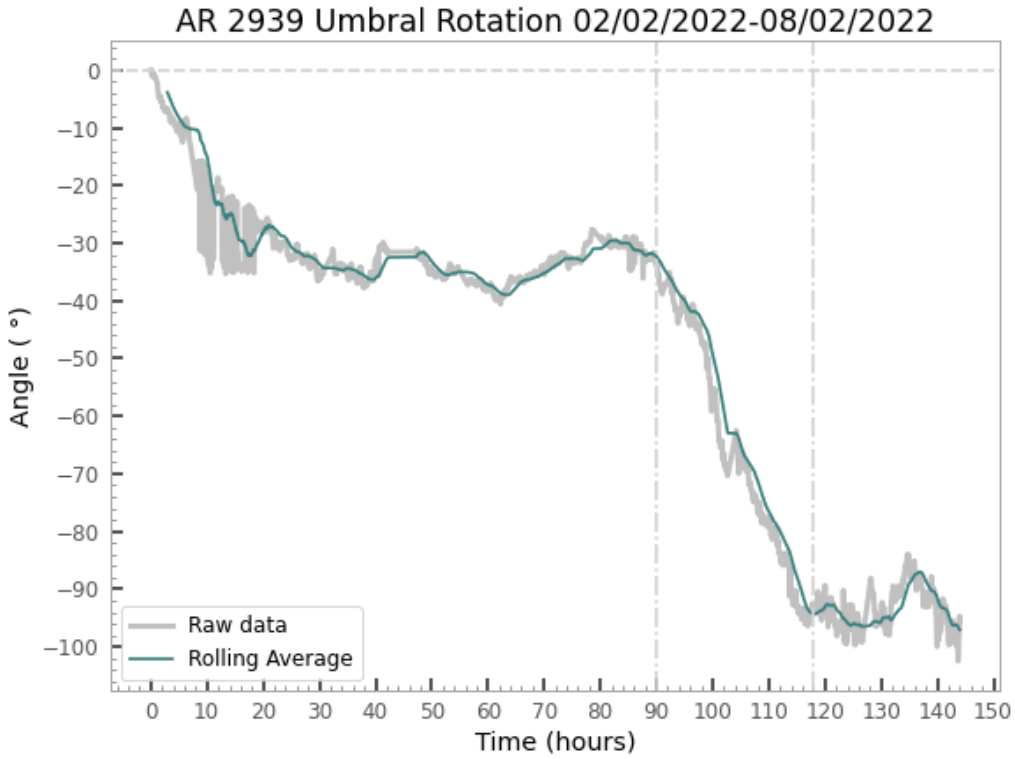

Figure 4.4-1 Umbral rotation profile

Figure 4.4-1 shows the cumulative rotation profile of the ellipse fitted to the umbral boundary plotted as a function of time in hours. While also largely exhibiting a counter clockwise rotation, it is quite clear that the umbra does not follow the same rotation profile of the penumbral counterpart, there begins to be hint of differential rotation going on. In the first instances of the analysis, the umbra describes a slowly decelerating counter clockwise motion, leading into a relatively quiescent period where very little rotation is measured up to 64h. Thereafter, a turning point on the plot reveals a reversal of the angular motion, describing a clockwise rotation up until 84h. The focus is drawn to the part of the graph outlined by the dot-dashed lines: A sudden reversal and harsh acceleration of the umbral rotation appears at 90h, which is then completely halted at 118h. This is precisely where when the solar flare event occurs. After the flare period, the umbra displays almost no rotation for another 15 hours. There is also a flare occurrence at 144h recorded on the flare data base, however these measurements are inclusive as the analysis ends then, though there may be a display of a repeating pattern. Unlike the dynamics of the penumbra, the complexity of the umbral rotation suggests an interaction, a causality, or at the least a correlation with the flare event recorded on the 6th February (118h from start of the analysis). The amount of detail achieved in these measurements is only possible due to the high polling rates, and would otherwise be overlooked using manual measurements. The erratic section of raw data in the beginning of the plot is due to the umbra being cleaved for 10 hours, proving a difficulty for the programme to properly determine the umbral boundaries.

ljt6@aber.ac.uk

5

Discussion & Future Work

The rotation rates of the umbral and penumbral areas of sunspot AR2939 were measured using continuum intensity images. This sunspot was associated with a C2 flare on the 6th February 13:06 UT. The flare was found to take place after an inversion and strong acceleration in the angular motion of the sunspot's umbra. Upon the flare event, the rotation was suddenly stopped. It was also found that the penumbra was seemingly unaffected by the umbral rotation. This differential rotation may constitute a straining/stressing mechanism on the flux tubes – which, coupled with the sharp increase in umbral rotation - may supply sufficient magnetic energy into the corona for solar eruptions to occur. The energy budgets of solar flares deserve further investigation. Understanding their origins may lead to great advances in the ability to predict such events. Furthermore, AR2939 was associated with a second C3 class flare on the 8th February 21:38 UT. Although entirely hypothetical and inconclusive, the increase and inversion in positive umbral rotation at 130-144h, may be an indication to the onset of this flare. If this is the case, there seems to be some repeating pattern prior to eruptive events. To confirm this idea, much more work and investigation of other flaring sunspots is needed. This project was the foundations for extensive research in the identification of sunspot dynamic patterns prior to flare onsets.

The sunspot analysed in this project served as a both a means of testing the performance of the approach, and to gather information on the sunspot activity prior to a flare event. Of course, it is pertinent to compare results obtained from these techniques to the results from previous literature to ascertain its proper performance. *Brown et al.*describes a method to calculate rotation of a sunspot by tracking fibrils and other radial features within the boundaries of a sunspot's penumbra. In his report, AR11147 was recorded from 17th to 25th January 2011. Their methods produced an absolute penumbral rotation of about 100°, in both clockwise and anti-clockwise direction. The first limitations come to light when comparing with our results. Firstly, in their paper, AR11147 was tracked within 60° of solar centre. At such positions, projection effects due to the sunspot not being at solar centre become non-negligible. For fair comparison, the same sunspot was tracked within 45° of solar centre. Ultimately however, the geometry of the sunspot was too circular to correctly measure rotation with the simplistic ellipse fitting method, at least without operations to deal with reprojection. Yet, a similar bulk rotation was measured, about 90° total rotation, albeit not describing the same profile as the *Brown et al.* methods.

The techniques presented in this report does a reasonable job of recording sunspot rotations, but in comparison to other methods, fails when given the task of measuring complex sunspot motion such as umbral clustering or cleaving. It should also be noted that the outcome of these methods, while reliable for small C-class flares and lower, it will become crucial to implement adaptive thresholding when dealing with more substantial events. Although subtle,

ljt6@aber.ac.uk

X-class flares have been observed to influence HMI continuum images, brightening the intensities of a sunspot's umbra. Moreover, the simple thresholding and ellipse fitting techniques require a 'well behaved' sunspot to produce an adequate rotation profile. A sunspot's good behaviour here is defined by a slightly elliptic geometry and a clear and steady umbra which displays no morphing or cleaving. Ultimately, these methods are extremely limited. However, such techniques can benefit from some extra work, which would have been achieved if time allowed for it. This would include cross-referencing each frame in sequence, to reduce error in measurements but to also allow accurate description of fast morphing umbra regions and cleaving umbral regions. From literature and visual observations, it is clear that in many instances before and during flare events, a sunspots umbra seems to split and counter-rotate. Another improvement that would lead to a more universal use of the programme is the ability to track umbral clusters independently.

6

Conclusion

The aim of this research was to identify a correlation between sunspot dynamics and nearby solar flares. This was achieved by writing a python programme that enabled the use of high polling rates offered by the SDO/HMI. The flaring sunspot AR2939 was pre-selected using Solar Demon Flare database and chosen for its adequate characteristics. The sunspot was tracked for 6 days at a cadence of 1 image every 3 minutes, then sent through a processing pipeline to extrapolate the umbral and penumbral rotation profiles. The umbral rotation seemed to either be the cause or was an effect of the flare phenomenon; prior to the flare event, the angular motion was suddenly inverted and accelerated for some period. Following the flare, the umbral rotation came to a total halt. This is a clear indication that there is some relationship between sunspot rotation and flare events, although the measurements are inconclusive and would require further investigation. On the other hand, the penumbra seemed to be unaffected by the harsh acceleration of the umbra, hinting at a differential rotation between both regions of the sunspot. In conjunction with the umbral acceleration, the differential rotations may sufficiently stress the sunspot's magnetic fluxes for an eruptive event to occur.

ljt6@aber.ac.uk

7

References

7.1 Literature Review References

1. Schmidt, W., *Magnetic field and dynamics of sunspots.* Solmag 2002: Proceedings of the Magnetic Coupling of the Solar Atmosphere Euroconference and Iau Colloquium 188, 2002. **505**: p. 167-174.
2. Kosovichev, A.G., *Subsurface characteristics of sunspots.* Solar Activity Cycle and Particle Acceleration, 2006. **38**(5): p. 876-885.
3. Hoppner, K. and M. Bittner, *Detection of solar activity signatures in OH* temperature fluctuations possibly related to the differential rotation of the Sun.* Journal of Atmospheric and Solar-Terrestrial Physics, 2009. **71**(12): p. 1287-1292.
4. Parker, E.N., *SUNSPOTS AND THE PHYSICS OF MAGNETIC-FLUX TUBES .1. GENERAL NATURE OF THE SUNSPOT.* Astrophysical Journal, 1979. **230**(3): p. 905-913.
5. Wang, H.M. and H. Zirin, *FLOWS AROUND SUNSPOTS AND PORES.* Solar Physics, 1992. **140**(1): p. 41-54.
6. Beckers, J.M. and E.H. Schröter, *The intensity, velocity and magnetic structure of a sunspot region.* Solar Physics, 1969. **10**(2): p. 384-403.
7. Meyer, F., H.U. Schmidt, and N.O. Weiss, *The stability of sunspots.* Monthly Notices of the Royal Astronomical Society, 1977. **179**(4): p. 741-761.
8. Hale, G.E., *On the Probable Existence of a Magnetic Field in Sun-Spots.* The Astrophysical Journal, 1908. **28**: p. 315.
9. Wang, H.M. and C. Liu, *Structure and evolution of magnetic fields associated with solar eruptions.* Research in Astronomy and Astrophysics, 2015. **15**(2): p. 145-174.
10. Zhang, M. and B.C. Low, *The Hydromagnetic Nature of Solar Coronal Mass Ejections.* Annual Review of Astronomy and Astrophysics, 2005. **43**(1): p. 103-137.
11. Kosovichev, A.G. and V.V. Zharkova, *Magnetic Energy Release and Transients in the Solar Flare of 2000 July 14.* The Astrophysical Journal, 2001. **550**(1): p. L105-L108.
12. Wang, H., et al., *Rapid Changes of Magnetic Fields Associated with Six X-Class Flares.* The Astrophysical Journal, 2002. **576**(1): p. 497-504.
13. Patterson, A. and H. Zirin, *Transient magnetic field changes in flares.* The Astrophysical Journal, 1981. **243**: p. L99.
14. Rausaria, R.R., et al., *THE VARIATION OF FILAMENT DIRECTION IN A FLARING REGION.* Solar Physics, 1993. **146**(1): p. 137-145.
15. Wang, S., C. Liu, and H.M. Wang. *Study of sunspot motion and flow fields associated with solar flares*. in *273th Symposium of the International-Astronomical-Union*. 2010. Ventura, CA.
16. Brown, D., Nightingale, R., Alexander, D. . and et al., *Observations of Rotating Sunspots from TRACE*. 2003.
17. Tian, L. and D. Alexander, *Role of sunspot and sunspot-group rotation in driving sigmoidal active region eruptions.* Solar Physics, 2006. **233**(1): p. 29-43.
18. Yan, X.L., et al., *The causality between the rapid rotation of a sunspot and an X3.4 flare.* Research in Astronomy and Astrophysics, 2009. **9**(5): p. 596-602.

ljt6@aber.ac.uk

19. Yan, X.L., Z.Q. Qu, and D.F. Kong, *Relationship between rotating sunspots and flare productivity.* Monthly Notices of the Royal Astronomical Society, 2008. **391**(4): p. 1887-1892.
20. Wang, R., et al., *Relationship Between Sunspot Rotation and a Major Solar Eruption on 12 July 2012.* Solar Physics, 2016. **291**(4): p. 1159-1171.
21. Ramesh, K.B., *CORONAL MASS EJECTIONS AND SUNSPOTS-SOLAR CYCLE PERSPECTIVE.* Astrophysical Journal Letters, 2010. **712**(1): p. L77-L80.
22. Gao, P.X., J.L. Xie, and J. Zhong, *Phase Relationships Between the CME-Energy Cycle, the Sunspot-Area Cycle and the Flare-Index Cycle.* Solar Physics, 2014. **289**: p. 1831.
23. Scherrer, P.H., et al., *The Helioseismic and Magnetic Imager (HMI) Investigation for the Solar Dynamics Observatory (SDO).* Solar Physics, 2012. **275**(1-2): p. 207-227.
24. Brown, D., *SDO primer.* 2010.
25. Gyori, L., *Automation of Tracking Various Sunspot Group Entities and Demonstrating Its Usage on the Flaring NOAA AR 11429.* Solar Physics, 2015. **290**(6): p. 1627-1645.
26. Györi, L., *Automation of Area Measurement of Sunspots.* Solar Physics, 1998. **180**(1): p. 109-130.
27. Brown, D. and A. Walker, *A Semi-Automatic Method to Measure the Rotation of Sunspots.* Solar Physics, 2021. **296**(3): p. 32.
28. Zheng, J.C., et al., *ON THE ROTATION OF SUNSPOTS AND THEIR MAGNETIC POLARITY.* Astrophysical Journal, 2016. **826**(1).
29. Permata, K. and D. Herdiwijaya. *The Measurement of Solar Differential Rotation from Proper Motion of Individual Sunspots*. in *10th Southeast-Asia-Astronomical-Network (SEAAN) Meeting*. 2018. Indonesia: Iop Publishing Ltd.
30. Leighton, R.B., R.W. Noyes, and G.W. Simon, *Velocity Fields in the Solar Atmosphere. I. Preliminary Report.* The Astrophysical Journal, 1962. **135**: p. 474.
31. Chaplin, W.J., et al., *The solar cycle as seen by low-ℓ p-mode frequencies: comparison with global and decomposed activity proxies.* Monthly Notices of the Royal Astronomical Society, 2004. **352**(4): p. 1102-1108.
32. Dziembowski, W.A. and P.R. Goode, *Sources of Oscillation Frequency Increase with Rising Solar Activity.* The Astrophysical Journal, 2005. **625**(1): p. 548-555.
33. Schunker, H., D.C. Braun, and P.S. Cally, *Surface magnetic field effects in local helioseismology.* Astronomische Nachrichten, 2007. **328**(3-4): p. 292-297.

7.2 Dissertation References

34. *Solar Demon Flare Detection* Available from: https://wwwbis.sidc.be/solardemon/science/flares.php?min_seq=1&min_flux_est=0.000001&days=0&science=1.
35. *SunPy DRMS* Available from: https://github.com/sunpy/drms.
36. Alexander, D. *Limb Darkening function IDL/SSW*. 14 Oct 1996; Available from: https://hesperia.gsfc.nasa.gov/ssw/gen/idl/solar/darklimb_correct.pro.
37. Cox, A.N., *Allen's astrophysical quantities*. 2000.
38. Grimes, R., B. Pintér, and H. Morgan, *Observation of Differential Rotation Within a Sunspot Umbra During an X-Class Flare.* Solar Physics, 2020. **295**(6): p. 87.
39. Fitzgibbon, A., M. Pilu, and R. Fisher, *Direct Least-squares fitting of ellipses*. Vol. 21. 1996. 253-257 vol.1.

ljt6@aber.ac.uk

8

Appendix

```
"""
Created on Sun Apr 10 11:30:56 2022

@author: Leif Tinwell
"""
import os
from os import listdir
import drms
import cv2
import gc
import numpy as np
import pandas as pd
from datetime import datetime
import matplotlib
import matplotlib.pyplot as plt
matplotlib.use('Agg')
plt.ioff()
from matplotlib.ticker import MultipleLocator
import sunpy.map
from astropy.io import fits
from astropy.visualization import astropy_mpl_style
plt.style.use(astropy_mpl_style)

    # ----------------------------------------------------------------------------

# initializing DRMS client to given email address
client = drms.Client(email = 'leiftinwell@rocketmail.com', verbose=True)

fits_dir = 'D:/Desktop/Uni/project/downloads/'
corrected = 'D:/Desktop/Uni/project/corrected/'
out_dir = 'downloads'

    # ----------------------------------------------------------------------------


"""
The HMI continuum data refers to the map of the continuum intensity of the solar
spectrum in the region of the Fe I absorption line @6173A on the surface of the
sun.
The continuum data is available in the DRMS series  hmi.Ic_45s and hmi.Ic_720s
Continuum data with Limb Darkening removed can be found in the DRMS series
hmi.Ic_noLimbDark_720s
"""

si = client.info('hmi.Ic_45s')                          #data series of interest
qstr = 'hmi.Ic_45s[2022.02.02_TAI-2022.02.08_TAI@3m]'       #start/end/cadence

print(f'Data export query:\n {qstr}\n')

process = {'im_patch':{     #construct dictionary specyfying the cutout request
    't_ref': '2011-01-21T07:16:35',
    't': 0,
    'r': 0,
    'c': 0,
```


ljt6@aber.ac.uk

```
    'locunits': 'arcsec',
    'boxunits': 'arcsec',
    'x': -20,
    'y': 469,
    'width': 50,
    'height': 50,
    }}


print('Submitting export request...')
result = client.export(     # Submit request using 'process' to define a cutout
    qstr,
    method = 'url',
    protocol='fits',
    email = 'leiftinwell@rocketmail.com',
    process = process,
    )

print(result)
print(f'\nRequest URL: {result.request_url}')                 #print request URL
print(f'{int(len(result.urls))} file(s) available for download.\n')
result.wait()
downloaded_file = result.download(out_dir)      #download file from request URLs
print('Download finished.')
print(f'\nDownload directory:\n "{os.path.abspath(out_dir)}"\n')


def image_manip():
    for filename in os.listdir(fits_dir):
        file = os.path.join(fits_dir, filename)
        if filename.endswith('.fits'):
            print(file)
            hmi_map = sunpy.map.Map(file)
            # hmi_map.plot(autoalign=True)
            hmi_map.peek()


"""
Once files for a given sunspot are downloaded, they need to be processed to
eliminate
the effects of Limb Darkening.

    Based on:
      https://hesperia.gsfc.nasa.gov/ssw/gen/idl/solar/darklimb_correct.pro

    Coefficients taken from
      Cox, A. N.: Allen's Astrophysical Quantities, Springer, 2000 taken from IDL
"""

def writefits(image):
    os.system("rm -r limbcorrect.fits")
    hdu = fits.PrimaryHDU(image)
    hdul = fits.HDUList([hdu])
    hdul.writeto('limbcorrected.fits')


def figure(image, title='image'):
    fig = plt.figure(figsize=(8,8), frameon=False)
    ax = plt.Axes(fig, [0., 0., 1., 1.])
    ax.set_axis_off()
    fig.add_axes(ax)
    plt.imshow(image, cmap = 'Greys_r',origin='lower')
    plt.savefig(title + ".png", dpi='figure')
    plt.close(fig)


def darklimb(array):
```


ljt6@aber.ac.uk

```
"""
Darklimb function:
    files need to be .FITS in order to take advantage of Header structure

Output:
    DOS array: First image is the corrected array, the second is the original.
"""

# ------------------------------------------------------------------------

def darklimb_u(ll):
    pll = np.array([1.0,ll,ll**2,ll**3,ll**4,ll**5])
    au = -8.9829751
    bu = 0.0069093916
    cu = -1.8144591e-6
    du = 2.2540875e-10
    eu = -1.3389747e-14
    fu = 3.0453572e-19
    aa=np.array([au,bu,cu,du,eu,fu])
    ul = sum(aa*pll)
    return ul

def darklimb_v(ll):
    pll = np.array([1.0,ll,ll**2,ll**3,ll**4,ll**5])
    av = 9.2891180
    bv = -0.0062212632
    cv = 1.5788029e-6
    dv = -1.9359644e-10
    ev = 1.1444469e-14
    fv = -2.599494e-19
    aa=np.array([av,bv,cv,dv,ev,fv])
    vl = sum(aa*pll)
    return vl

# ------------------------------------------------------------------------

#Read data files
data = fits.getdata(name, 1)
head = fits.getheader(name, 1)

#Parameters needed for the function
wavelength = head['WAVELNTH'] # Wavelength
xcen = head['CRPIX1'] # X center
ycen = head['CRPIX2'] # Y center
radius = head['RSUN_OBS']/head['CDELT1'] # Pixels result
size = head['NAXIS1'] # X array size

ll = 1.0*wavelength

array = np.array(data) # convert data into np array
NaNs = np.isnan(array) # look for NaNs
array[NaNs] = 0.0      # Make all NaNs = 0

#Apply correction
ul = darklimb_u(ll)
vl = darklimb_v(ll)

xarr = np.arange(0,size,1.0) # Make X array
yarr = np.arange(0,size,1.0) # Make Y array
xx, yy = np.meshgrid(xarr, yarr) # Make XY array
# z: make array so that the zero center is the XY center
# Make circle
z = np.sqrt((xx-xcen)**2 + (yy-ycen)**2)
# grid: Normalize the circle so that inside radius is the unity
grid = z/radius
out = np.where(grid>1.0) # Look for the values greater than unity
```


ljt6@aber.ac.uk

```
    grid[out] = 0.0 # Make zero all those values (Domain of arcsin)

    limbfilt =  1.0-ul-vl+ul*np.cos(np.arcsin(grid))+vl*np.cos(np.arcsin(grid))**2

    # Final image
    imgout = np.array(array/limbfilt)

    return imgout, array

    # ----------------------------------------------------------------------

for filename in os.listdir(fits_dir):
    name = os.path.join(fits_dir, filename)
    print(name)
    new_name = 'corrected/' + str(filename)
    corrected, original = darklimb(name)
    figure(corrected, title = new_name)

"""
In order for the rotation of the sunspot to be measured, umbral and penumbral
boundaries are determined by using a combination of Gaussian blurs
and intensity thresholds. Thresholds are then used to contruct umbral/penumbral
boundaries, which are themselves used to compute the center of mass of the sunspot.
An ellipse is fitted to the contours.
The angle of rotation is computed using the coordinates of the
semi-major axis. Iterated for each image of the sequence and plotted as a rotation
profile over time.
"""


penumbra_angle_data = []
umbra_angle_data = []                                   #initializing variables
umbra_angle_dataUB = []
umbra_angle_dataMB = []
umbra_angle_dataLB = []
time_data = []
cpad = []
cuad= []
cpad1 = []
cuad1= []
cpad2 = []
cuad2= []
cpad3 = []
cuad3= []
Parea = []
Uarea = []
area_val1 = []
area_val2 = []
area_val3 = []


def grab_time_data():
    for filename in os.listdir('D:/Desktop/Uni/project/AR2939/.FITS Data/'):
        name = os.path.join('D:/Desktop/Uni/project/AR2939/.FITS Data/', filename)
        hdulist = fits.open(name)
        hdu = hdulist[1]
        t_rec = drms.to_datetime(hdu.header['T_REC'])
        time_data.append(t_rec)

def thresh_val():
    datamean_result = client.query(      #query DATAMEAN for each image in sequence
    qstr,key=['DATAMEAN'])
    dtm = pd.DataFrame(datamean_result)
    print(dtm)
    datamean = dtm.mean()
    print(f'datamean mean: {datamean}')
    IUmbral_UB = 0.55*datamean
```


ljt6@aber.ac.uk

```
    IUmbral_LB = 0.125*datamean
    IPenumbral_UB = 1.30*datamean
    IPenumbral_LB = 0.6*datamean
    val = {'umbra upper bound': IUmbral_UB,
           'umbra lower bound': IUmbral_LB,
           'penumbral upper bound': IPenumbral_UB,
           'penumbral lower bound': IPenumbral_LB
           }
    return val
I = thresh_val()
Umbral_lowerbound = I['umbra lower bound']/255
Umbral_upperbound = I['umbra upper bound']/255
Umbral_MB = Umbral_lowerbound*2
Penumbral_lowerbound = I['penumbral lower bound']/255
Penumbral_upperbound = I['penumbral upper bound']/255
print(f'\n Umbral lower bound: {Umbral_lowerbound} \n',
      f'\n Umbral upper bound: {Umbral_upperbound} \n',
      f'\n Penumbral lower bound: {Penumbral_lowerbound} \n',
      f'\n Penumbral upper bound: {Penumbral_upperbound} \n'
      )

def penumbra_ellipse_fitting():
    for filename in os.listdir('D:/Desktop/Uni/project/AR2939/Image Data/'):
        file = os.path.join('D:/Desktop/Uni/project/AR2939/Image Data/', filename)
        im = cv2.imread(file)                          #collect files from directory
        imgray = cv2.cvtColor(im, cv2.COLOR_BGR2GRAY)       #convert to grayscale
        blur = cv2.GaussianBlur(imgray, (45,45),55)
        #threshold to eliminate excess data, focus on penumbra area of sunspot
        threshold = cv2.threshold(blur, 215, 255, cv2.THRESH_BINARY_INV)[1]
          #find contours of threshold silhouette
        contours = cv2.findContours(threshold,
                                    cv2.RETR_EXTERNAL,
                                    cv2.CHAIN_APPROX_NONE
                                    )
        contours = contours[0] if len(contours) == 2 else contours[1]
        big_contour = max(contours, key=cv2.contourArea)
        area = cv2.contourArea(big_contour)
        Parea.append(area)
        ellipse = cv2.fitEllipse(big_contour)       #fit ellipse around contours
        (xc,yc),(d1,d2),anglep = ellipse
        result = im.copy()
        cv2.ellipse(result, ellipse, (0, 255, 0), 1)
        xc, yc = ellipse[0]
        cv2.circle(result, (int(xc),int(yc)), 1, (255, 255, 255), -1)#center dot
        penumbra_angle_data.append(anglep)        #send angle data to angle_data

def umbra_ellipse_fitting():
    for filename in os.listdir('D:/Desktop/Uni/project/AR2939/Image Data/'):
        file = os.path.join('D:/Desktop/Uni/project/AR2939/Image Data/', filename)
        im = cv2.imread(file)                          #collect files from directory
        imgray = cv2.cvtColor(im, cv2.COLOR_BGR2GRAY)       #convert to grayscale
        blur = cv2.GaussianBlur(imgray, (25,25), 25)
        #threshold to eliminate excess data, focus on penumbra area of sunspot
        threshold = cv2.threshold(blur, 120, 255, cv2.THRESH_BINARY_INV)[1]
        #find contours of threshold silhouette
        contours = cv2.findContours(threshold,
                                    cv2.RETR_TREE,
                                    cv2.CHAIN_APPROX_NONE
                                    )
        contours = contours[0] if len(contours) == 2 else contours[1]
        big_contour = max(contours, key=cv2.contourArea)
        area = cv2.contourArea(big_contour)
        Uarea.append(area)
        ellipse = cv2.fitEllipse(big_contour)       #fit ellipse around contours
        (xc,yc),(d1,d2),angleu = ellipse
        result = im.copy()
        cv2.ellipse(result, ellipse, (0, 255, 0), 1)
```


ljt6@aber.ac.uk

```
        xc, yc = ellipse[0]
        cv2.circle(result, (int(xc),int(yc)), 1, (255, 255, 255), -1)#center dot
        umbra_angle_data.append(angleu)         #send angle data to angle_data


#     # ------------------------------------------------------------------------

grab_time_data()
time_since_start = []
date_format = '%Y-%m-%d %H:%M:%S'
for i in time_data:
    t0 = datetime.strptime(str(time_data[0]), date_format)
    ti = datetime.strptime(str(i), date_format)
    td = ti - t0
    tdm = td.total_seconds() / 3600
    time_since_start.append(tdm)

    # ------------------------------------------------------------------------

penumbra_ellipse_fitting()
#cumulative rotation starting from 0
for i in penumbra_angle_data:
    a0 = float(penumbra_angle_data[0])
    ai = float(i)
    ca = ai - a0
    cpad.append(ca)
cpad = pd.Series(cpad)
prp = cpad.rolling(60)
prpm = prp.mean()

umbra_ellipse_fitting()
#cumulative rotation starting from 0
for i in umbra_angle_data:
    a0 = float(umbra_angle_data[0])
    ai = float(i)
    ca = ai - a0
    cuad.append(ca)
cuad = pd.Series(cuad)
urp = cuad.rolling(20)
urpm = urp.mean()

    # ------------------------------------------------------------------------
fig, ax1 = plt.subplots(constrained_layout=True)
ax1.set(title='AR 2939 area plot 02/02/2022-08/02/2022')
ax1.plot(time_since_start, Uarea, color='#39817f', label='Umbral area')
ax1.plot(time_since_start, Parea, color='#a9c12a', label='Penumbral area')
ax1.set_xlabel('Time (hours)')
ax1.set_ylabel('Area (pixels)')
ax1.minorticks_on()
ax1.xaxis.set_major_locator(MultipleLocator(10))
ax1.xaxis.set_minor_locator(MultipleLocator(2))
ax1.xaxis.grid(False)
ax1.yaxis.grid(False)
ax1.tick_params(which='major', width=2)
ax1.tick_params(which='major', length=7)
ax1.tick_params(which='minor', length=3)
ax1.legend(loc='upper right')
fig.savefig('AR2939UPA120215.png', dpi='figure')

    # ------------------------------------------------------------------------

fig, ax2 = plt.subplots(constrained_layout=True)
ax2.set(title='AR 2939 Penumbral Rotation 02/02/2022-08/02/2022')
ax2.plot(time_since_start, cpad, color='gainsboro', label='Raw Data', linewidth=3)
ax2.plot(time_since_start, prpm, color='#a9c12a', label='Rolling Average')
plt.axhline(y=0, color='lightgray', linestyle='--')
```


ljt6@aber.ac.uk

```
ax2.set_xlabel('Time (hours)')
ax2.set_ylabel('Angle ( °)')
ax2.minorticks_on()
ax2.xaxis.set_major_locator(MultipleLocator(10))
ax2.xaxis.set_minor_locator(MultipleLocator(2))
ax2.yaxis.set_major_locator(MultipleLocator(10))
ax2.yaxis.set_minor_locator(MultipleLocator(2))
ax2.xaxis.grid(False)
ax2.yaxis.grid(False)
ax2.tick_params(which='major', width=2)
ax2.tick_params(which='major', length=7)
ax2.tick_params(which='minor', length=3)
ax2.legend(loc='lower left')
fig.savefig('AR2939PR.png', dpi='figure')

    # ----------------------------------------------------------------------

fig, ax1 = plt.subplots(constrained_layout=True)
ax1.set(title='AR 2939 Umbral Rotation 02/02/2022-08/02/2022')
ax1.plot(time_since_start, cuad, color='silver', label='Raw data', linewidth=3)
ax1.plot(time_since_start, urpm, color='#39817f', label='Rolling Average')
plt.axhline(y=0, color='lightgray', linestyle='--')
plt.axvline(x=90, color='lightgray', linestyle='dashdot')
plt.axvline(x=118, color='lightgray', linestyle='dashdot')
ax1.set_xlabel('Time (hours)')
ax1.set_ylabel('Angle ( °)')
ax1.minorticks_on()
ax1.xaxis.set_major_locator(MultipleLocator(10))
ax1.xaxis.set_minor_locator(MultipleLocator(2))
ax1.yaxis.set_major_locator(MultipleLocator(10))
ax1.yaxis.set_minor_locator(MultipleLocator(2))
ax1.xaxis.grid(False)
ax1.yaxis.grid(False)
ax1.tick_params(which='major', width=2)
ax1.tick_params(which='major', length=7)
ax1.tick_params(which='minor', length=3)
ax1.legend(loc='lower left')
fig.savefig('AR2939UR.png', dpi='figure')
```


ljt6@aber.ac.uk